X-Ray Phase Contrast Imaging with Photon-Counting Detectors

Ke Li, PhD

Department of Medical Physics and Department of Radiology
University of Wisconsin-Madison

DEPARTMENTS OF Medical Physics & Radiology
UNIVERSITY OF WISCONSIN SCHOOL OF MEDICINE AND PUBLIC HEALTH

Grating-Based X-Ray Phase Contrast Imaging

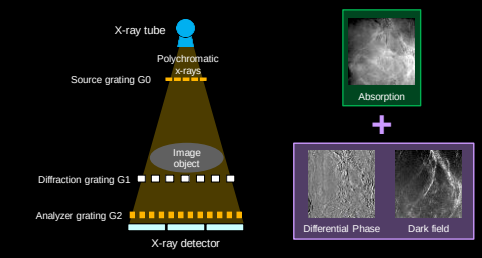

Prototype System at UW-Madison

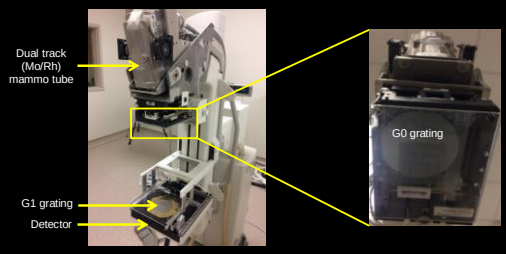

Prototype System at UW-Madison

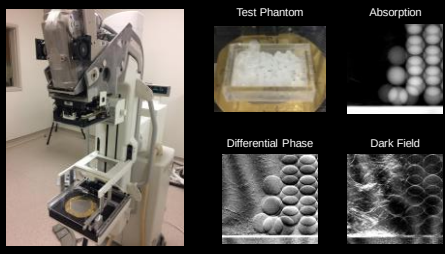

X-Ray Refraction and Small Angle Scattering

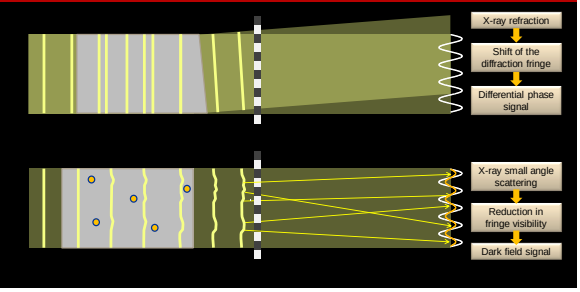

But how does a coarse detector element resolve tiny changes in the diffraction fringe pattern?

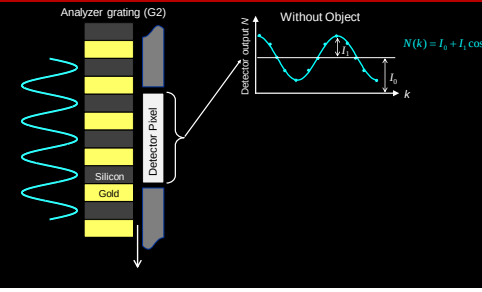

But how does a coarse detector element resolve tiny changes in the diffraction fringe pattern?

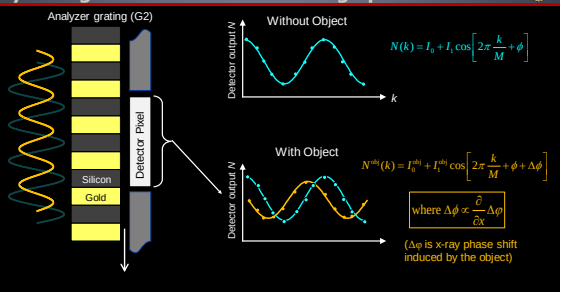

X-Ray Phase Shift

$$\Delta\varphi = -\frac{2\pi}{\lambda}\int_L \delta \mathrm{d}l \qquad \delta = \frac{r_0\lambda^2\rho_e}{2\pi}$$

$$\Delta\varphi = -r_0\lambda\int_L \rho_e \mathrm{d}l = -r_0\lambda\rho_e L$$

If $L = \frac{\pi}{r_0\lambda\rho_e}$, then $\Delta\varphi = -\pi$

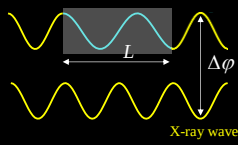

$\Delta\varphi$: x-ray phase shift
λ: x-ray wave length
δ: decrement in real part of refractive index
ρ_e: electron density
r_0: classical electron radius
L: object thickness

π-Phase Diffraction Grating for 32 keV X-Rays

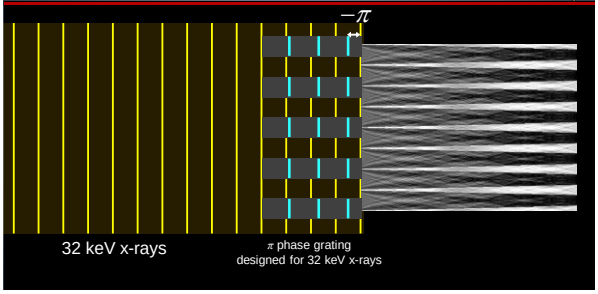

What would happen if the x-ray energy deviate from the designed operating energy?

- The structure height of the grating (L) was set so that for 32 keV x-rays:

$$\Delta\varphi_{32\mathrm{keV}} = -r_0\rho_e L\lambda_{32\mathrm{keV}} = -\pi$$

- Then for the same grating (same L and ρ_e), when the x-ray energy is16 keV

$$\Delta\varphi_{16\mathrm{keV}} = -r_0\rho_e L\lambda_{16\mathrm{keV}} = -r_0\rho_e L(2\lambda_{32\mathrm{keV}}) = -2\pi$$

~~π-Phase Diffraction Grating for 32 keV X-Rays~~
2π-Phase Grating for 16 keV X-Rays

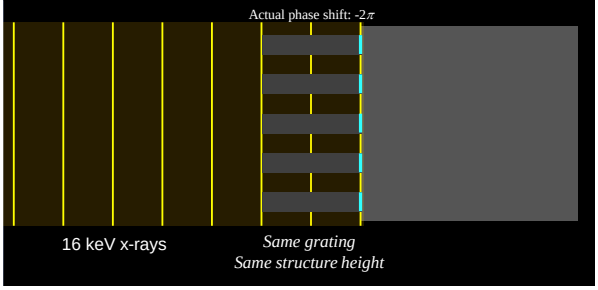

Diffraction Pattern with Polychromatic Source

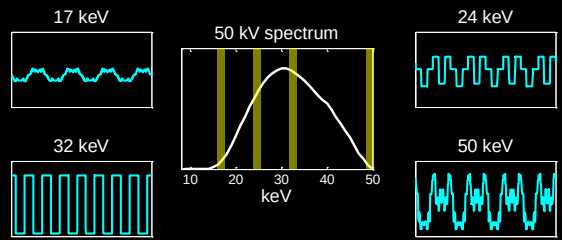

Diffraction Pattern with Polychromatic Source

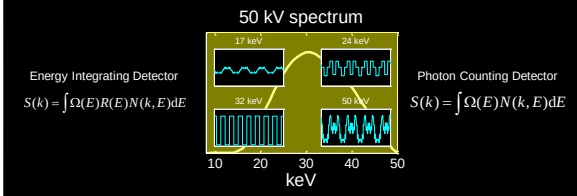

Energy Integrating Detector

$$S(k) = \int \Omega(E) R(E) N(k,E) \mathrm{d}E$$

Photon Counting Detector

$$S(k) = \int \Omega(E) N(k,E) \mathrm{d}E$$

$S(k)$: Detector signal at the kth phase step
$N(k)$: Number of x-ray photons at the kth phase step
$\Omega(E)$: X-ray spectrum
$R(E)$: Detector energy response function

Diffraction Pattern with Polychromatic Source: EID vs. PCD

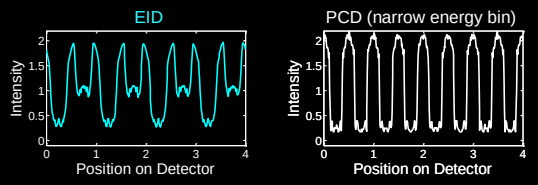

Diffraction Efficiency with Polychromatic X-Rays

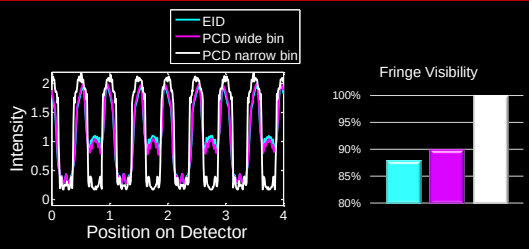

Energy-Dependent Interferometer Performance: Experimental Demonstration

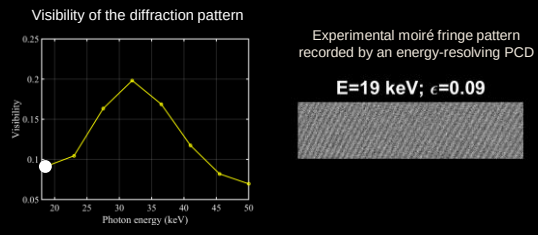

Energy-Dependent Interferometer Performance: Experimental Demonstration

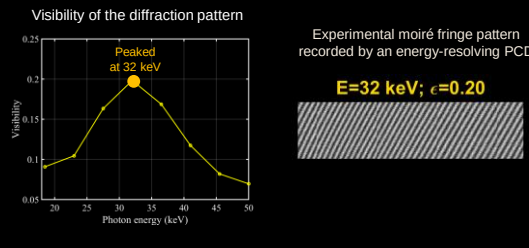

Impact to Phase Contrast Image Quality

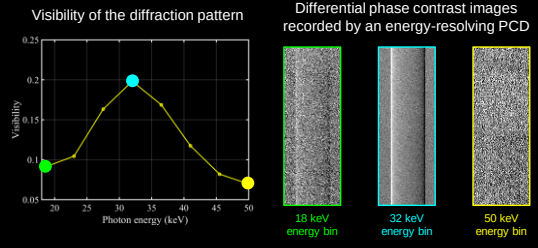

DPC Imaging with Energy-Integrating Detector

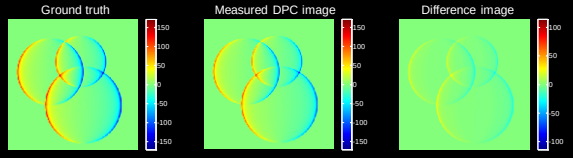

Reduction of Bias using Energy-Resolving PCD

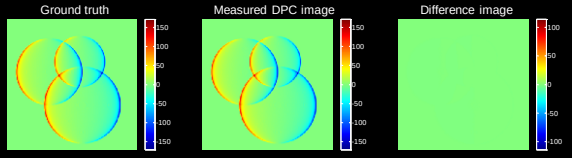

Energy Dependence of the Differential Phase Signal

- Differential phase contrast image signal ϕ is related to the energy by

$$\phi(x,y,E) = -\frac{\alpha}{E^2}\frac{\partial}{\partial x}\int_l \rho_e(x,y,z)dz \quad \text{..... (1)}$$

where numerical factor α is independent of x-ray energy E.

- Define $\varphi(x,y) \equiv -\alpha\frac{\partial}{\partial x}\int_l \rho_e(x,y,z)dz$
- Equation (1) becomes $\phi(x,y,E) = \frac{1}{E^2}\times\varphi(x,y)$

Spatial-Spectral DPC Image Matrix

$\phi(x,y,E) = \frac{1}{E^2}\times\varphi(x,y)$

Rank (J) = 1

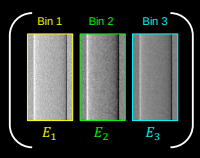

$$J = \begin{bmatrix} \frac{1}{E_1^2}\times\varphi(x_1,y_1) & \frac{1}{E_2^2}\times\varphi(x_1,y_1) & \frac{1}{E_3^2}\times\varphi(x_1,y_1) \\ \frac{1}{E_1^2}\times\varphi(x_1,y_2) & \frac{1}{E_2^2}\times\varphi(x_1,y_2) & \frac{1}{E_3^2}\times\varphi(x_1,y_2) \\ \vdots & \vdots & \vdots \\ \frac{1}{E_1^2}\times\varphi(x_m,y_n) & \frac{1}{E_2^2}\times\varphi(x_m,y_n) & \frac{1}{E_3^2}\times\varphi(x_m,y_n) \end{bmatrix}$$

The number of rows in J is determined by number of image pixels, and the number of columns in J is determined by the number of energy bins

Y. Ge, *et al.*, Vol. 24, Issue 12, pp. 12955-12968, Opt. Exp. (2016)

Rank-One Approximation

$$J = U\Sigma V^T = \sum_{i=1}^{N}\sigma_i\overrightarrow{u_i}\otimes\overrightarrow{v_i}^T \approx \sigma_1\overrightarrow{u_1}\otimes\overrightarrow{v_1}^T$$

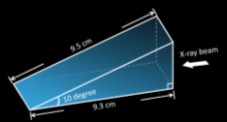

The wedge phantom provides a constant x-ray refraction angle

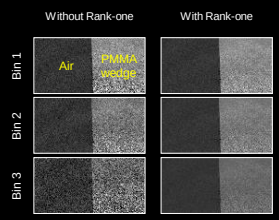

Y. Ge, *et al.*, Vol. 24, Issue 12, pp. 12955-12968, Opt. Exp. (2016)

Noise Power Spectrum (NPS) Analysis

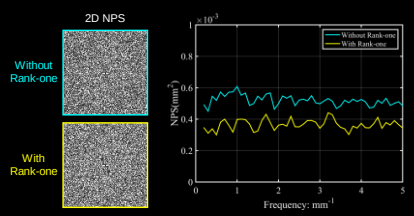

CNR Improvement using Rank-One Approximation

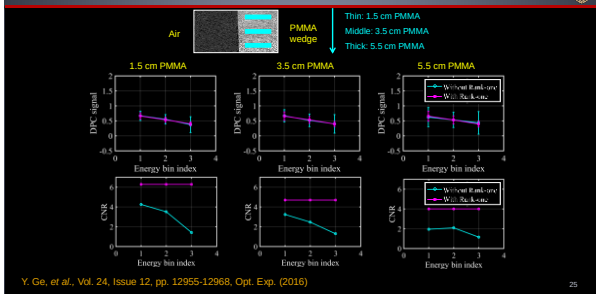

Y. Ge, *et al.*, Vol. 24, Issue 12, pp. 12955-12968, Opt. Exp. (2016)

25

Impacts of Detector Electronic Noise in Multi-Contrast Imaging: Cascaded Systems Analysis

$$\langle I^{(k)} \rangle = \boxed{I_0} + \boxed{I_1} \cos\left[2\pi \frac{k}{M} + \boxed{\varphi} \right]$$

Absorption Dark field Differential phase

$$\langle I_0 \rangle = \frac{1}{M} \sum_{k=1}^{M} \langle I^{(k)} \rangle$$

$$\langle I_1 \rangle = \frac{2}{M} \sqrt{\left[\sum_{k=1}^{M} \langle I^{(k)} \rangle \sin\left(\frac{2\pi k}{M} \right) \right]^2 + \left[\sum_{k=1}^{M} \langle I^{(k)} \rangle \cos\left(\frac{2\pi k}{M} \right) \right]^2}$$

$$\langle \varphi \rangle = \tan^{-1}\left[\frac{\sum_{k=1}^{M} \langle I^{(k)} \rangle \sin\left(\frac{2\pi k}{M} \right)}{\sum_{k=1}^{M} \langle I^{(k)} \rangle \cos\left(\frac{2\pi k}{M} \right)} \right]$$

Estimator

$I^{(k)} = \langle I^{(k)} \rangle + \text{noise}$

Input

$I_0 = \langle I_0 \rangle + \text{noise}$
$I_1 = \langle I_1 \rangle + \text{noise}$
$\varphi = \langle \varphi \rangle + \text{noise}$

Output

Impacts of Detector Electronic Noise: Results of Cascaded Systems Analysis

ε: Fringe visibility
I^{Σ}: Total exposure
M: Total number of phase steps

Phase

$$\sigma_{\varphi}^2 = \frac{1}{\varepsilon^2 \langle I^{\Sigma} \rangle^2} \left[2k \langle I^{\Sigma} \rangle + \cancel{2M\sigma_e^2} \right]$$

$$\sigma_{I^k}^2 = \sigma_{\text{quantum}}^2 + \cancel{\sigma_e^2} = k \langle I^k \rangle + \cancel{\sigma_e^2}$$

Noise of detector output

$$\sigma_{I_1}^2 = \frac{2k \langle I^{\Sigma} \rangle}{M^2} + \cancel{\frac{2\sigma_e^2}{M}}$$

Dark Field

$$\sigma_{I_0}^2 = \frac{k \langle I^{\Sigma} \rangle}{M^2} + \cancel{\frac{\sigma_e^2}{M}}$$

Absorption

Impacts of Electronic Noise Rejection: Experimental Studies

Photon counting detector (PCD)

Energy integrating detector (EID)

Detector type	Single photon counting	Energy integrating
Model	XCounter XC-FLITE X-1	Shad-o-Box 2048
Pixel size	100 µm	96 µm (after 2 x 2 binning)
Detector active area	15.5 cm x 1.3 cm	10 cm x 5 cm
Conversion method	Direct	Indirect
Conversion material	CdTe	Gd_2O_2S
Maximum frame rate	1000 fps	2.7 fps
Readout chip	CMOS	CMOS
Bit depth	12	12
kV range	5-300	10-160

X Ji, et al., "Energy Calibration of Photon Counting Detectors Based On Measurement of X-Ray Attenuation Curve of K-Edge Materials."
Wednesday, 7:30 AM - 9:30 AM Room: 601

Impacts of Electronic Noise: Tomosynthesis Images

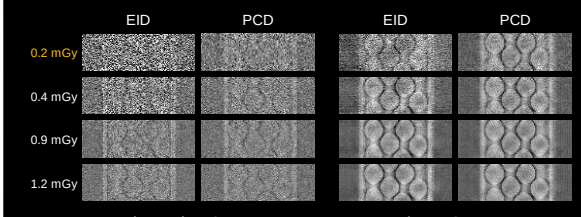

Impacts of Electronic Noise: CT Images

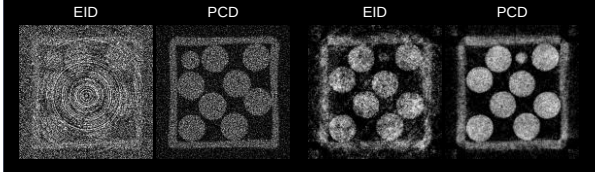

Additional Benefit of PCD: Improvement in Detector DQE(*f*)

Comparing PCD with EID #1 (thin scintillator):
PCD has slightly better MTF and much better DQE

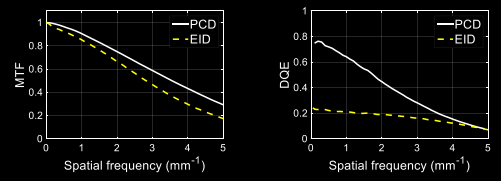

Additional Benefit of PCD: Improvement in Detector Spatial Resolution

Comparing PCD with EID #2 (thick columnar scintillator):
Similar DQE, but PCD has much better MTF

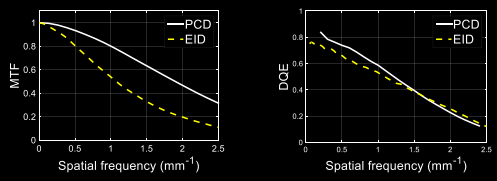

Phase Contrast Images of ACR Mammography Accreditation Phantom

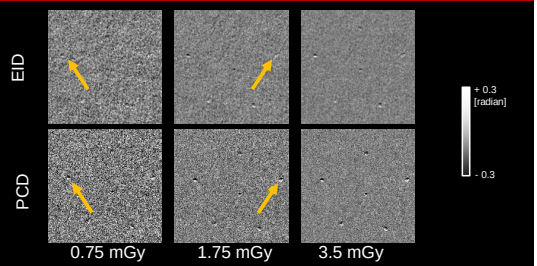

Xu *et al.*, RSNA 2016

Images of In-house Phantom

Absorption contrast
clinical mammo system
1.84 mGy

Phase contrast
PCD
1.75 mGy

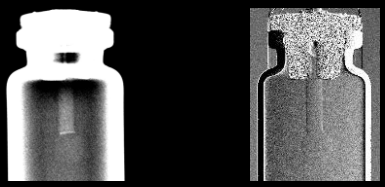

Xu *et al.*, RSNA 2016

Experimental Results of In-house Phantom

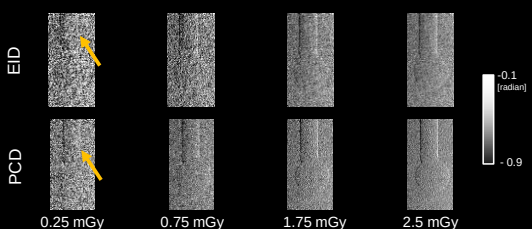

Xu *et al.*, RSNA 2016

Improvement in Ideal Observer Performance using PCD

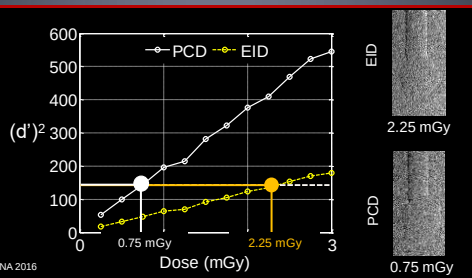

Xu *et al.*, RSNA 2016

Discussion and Conclusion

- Performance of x-ray phase contrast imaging (XPCI) is sensitive to x-ray energy
  - Visibility of x-ray diffraction fringes is highest at designed operating energy; it may drop significantly at other energy levels
  - Consequently, the use of polychromatic x-rays decreases fringe visibility
  - Accuracy of the estimated phase contrast signal is highest with monochromatic x-rays
- Performance of XPCI is also sensitive to electronic noise accumulated over multiple phase steps
- Similar to conventional x-ray imaging, performance of XPCI strongly depends on detector DQE

Discussion and Conclusion

- Compared with conventional energy-integrating detectors, photon counting detectors have major advantages in x-ray phase contrast imaging
  - The energy resolving capability of PCD offers the freedom of
    - Selectively utilize a narrow energy window to boost the diffraction efficiency of the grating interferometer, or
    - Jointly utilize all energy windows to boost signal-to-noise ratio
  - Rejection of electronic noise accumulated over multiple phase steps significantly improves phase contrast image quality, especially at low radiation exposure levels
  - Improved DQE offered by PCD leads to better image quality or radiation dose efficiency

Discussion and Conclusion

- The extent to which PCD benefits phase contrast imaging strongly depends on its energy resolution
- Emerging technologies such as anti-charge sharing could provide significant energy resolution improvement
- Further developments in PCD technologies could further improve phase contrast imaging performance

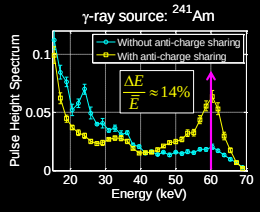

Americium-241: courtesy of UW Cyclotron Group

Acknowledgements

- Dr. Guang-Hong Chen
- Dr. Ran Zhang
- Dr. Yongshuai Ge
- Dr. John Garrett
- Xu Ji

- Funding support
  - NIH R01EB020521
  - DOD Breakthrough Award W81XWH-16-1-0031

Thank You